Proc. Natl. Acad. Sci. USA
Vol. 86, pp. 7336–7340, October 1989
Biochemistry

Geometry of a branched DNA structure in solution

(Holliday structure/recombination/DNA curvature/birefringence decay/gel electrophoresis)

JULIA PROMISEL COOPER AND PAUL J. HAGERMAN*

Department of Biochemistry, Biophysics, and Genetics, University of Colorado Health Sciences Center, Denver, CO 80262

Communicated by Robert L. Baldwin, June 26, 1989

ABSTRACT **An approximate geometry of a stable, four-way DNA junction has been determined in free solution by applying the technique of transient electric birefringence. The current approach consists of (*i*) construction of a set of six molecules in which two of the four arms of a synthetic junction are elongated by approximately 9-fold (in each of the six possible two-arm combinations), (*ii*) determination of the ratios of the longest birefringence decay time of each elongated junction to the decay time of a linear control molecule, and (*iii*) comparison of the experimental ratios with corresponding ratios computed as a function of the junction interarm angle. The result is a set of six angles that define the geometry of the junction. In the presence of magnesium ions, the junction adopts a geometry in which particular pairs of arms approach colinearity. Furthermore, the geometry of the junction is significantly altered in the absence of magnesium, adopting a more uniform structure, although such an effect is not apparent on gels. The application of transient electric birefringence, as described in the current study, should be useful for the characterization of a broad range of tertiary structures in both DNA and RNA.**

Branched DNA molecules have been invoked as key intermediates in general genetic recombination (1–4). These branched intermediates, known as Holliday structures (junctions), consist of two homologous double helices joined by a crossed-strand exchange. Regeneration of duplex DNA from Holliday junctions occurs through their cleavage by specific endonucleases that do not demonstrate any strong sequence-dependence at the points of cleavage (5–11), thus suggesting that junction geometry plays an important role in directing the cleavage events. Unfortunately, natural Holliday structures are inherently difficult to study, due to their transient nature (a consequence of branch migration). An experimental model for branched recombination intermediates that avoids this problem, the synthetic DNA four-way junction, was developed by Seeman and Kallenbach (12, 13). Synthetic junctions can be designed to lack the sequence symmetry necessary for branch migration; stable formation of these so-called immobile junctions has been demonstrated using electrophoretic, thermal, and chromatographic analyses (10, 14, 15). Moreover, nuclear magnetic resonance studies have shown that base pairing occurs at the junction branch point (16). The synthetic four-way junction, therefore, represents a stable model system for investigating the geometries of branched DNA molecules.

We have reported (15) a gel electrophoretic analysis of the geometry of a synthetic, DNA four-way junction. That approach, which was based on the observation that bent DNA molecules exhibit reduced electrophoretic mobilities in polyacrylamide gels (17–19), involved the attachment of a relatively long DNA fragment ("reporter fragment") to two of the four arms of the junction, in each of six possible two-arm combinations; the electrophoretic mobilities of the extended junctions (J_{ex}) were then compared. In that study, several models for junction geometry (each having interarm angles that are independent of base sequence) were excluded on the basis of the electrophoretic behavior of the two-arm-extended structures. Quantitative structural conclusions based on gel studies are not warranted, however, until two issues have been addressed (15). (*i*) The relationship between the extent of gel retardation and the magnitude of bending has not been established. (*ii*) The extent to which the relative mobilities of J_{ex} might be affected by the surrounding gel matrix is unknown. Evaluation of either of these issues would be extremely difficult in the absence of information regarding the interarm angles in free solution. Therefore, we have sought to obtain such information in the present work.

In the current study, the method of transient electric birefringence (TEB; see refs. 20–23) has been used to determine the geometry of a particular DNA four-way junction (15). In brief, TEB involves the orientation of DNA molecules in solution in response to a brief electric field pulse; the resulting solution is optically anisotropic and is monitored using polarization-dependent refraction (birefringence). After removal of the field, the solution again becomes optically isotropic, the rate of return being a sensitive function of DNA length and configuration (18, 21). For DNA molecules of the same contour length, a more bent molecule will experience more rapid rotational diffusion and thus will manifest a smaller rotational decay time. The rotational decay times of all six J_{ex} have, therefore, been compared with that of an appropriate linear control (LC) molecule. Using a computational method for determining relative birefringence decay times as a function of bend angle, we have determined the angles included by all six pairs of junction arms in solution and have ascertained that the relationship between electrophoretic retardation and degree of bending is not rigorously monotonic for junction-containing fragments.

MATERIALS AND METHODS

Synthesis and Purification of the Four-Way Junction and LC Oligomer. Protocols for the production of synthetic oligonucleotides (Fig. 1) were essentially as described (15). The stability of the junction under conditions used for TEB studies was assessed by examining its melting behavior in 10 mM Tris·HCl (pH 8.0; 0–60°C). Thermal melting curves were performed on a Cary 219 spectrophotometer with an indwelling temperature probe; temperature was increased at a rate that did not exceed 0.3°C/min. For a total junction concentration of 10 μg/ml (two 30-mers and two 26-mers, previously annealed), the thermal transition midpoint was 36°C, with a fractional hyperchromic change of <2% below 15°C. Moreover, the stability of the junction increases, as expected, upon addition of 1 mM $MgCl_2$.

The publication costs of this article were defrayed in part by page charge payment. This article must therefore be hereby marked "*advertisement*" in accordance with 18 U.S.C. §1734 solely to indicate this fact.

Abbreviation: J_{ex}, extended junction(s); TEB, transient electric birefringence; LC, linear control.

*To whom reprint requests should be addressed.

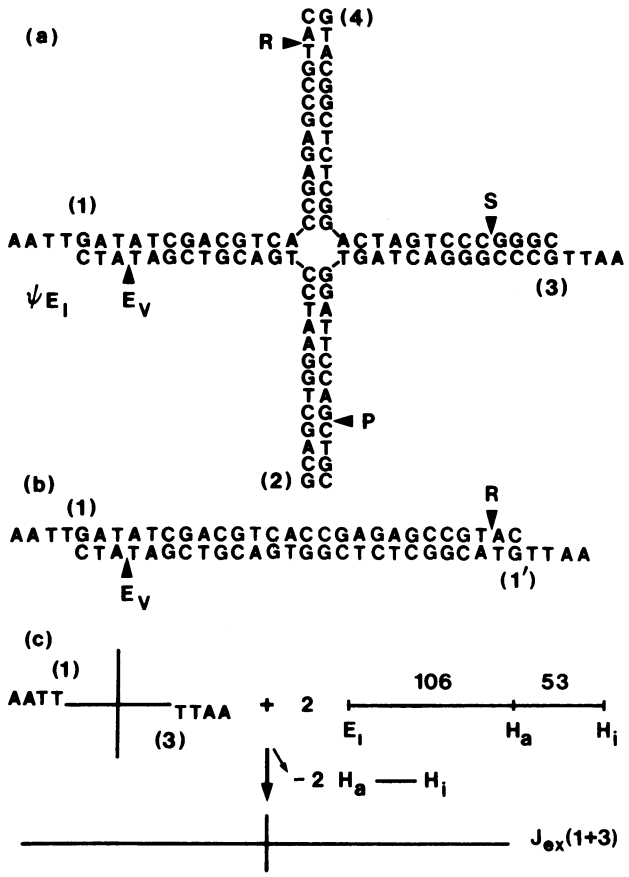

FIG. 1. (*a*) Sequence of the synthetic DNA four-way junction used for the current study. The numeric designation of a particular junction arm corresponds to the oligonucleotide core sequence whose 5′ end resides in that arm. The junction pictured represents the precursor for the J_{ex}, $J_{ex}(1+3)$, in which arms 1 and 3 are each elongated by 106 base pairs (bp). The innermost 4 bp in each arm were adapted from the junction designed by Seeman and Kallenbach (13). (*b*) Sequence of the 30-bp molecule used for the LC. The core of the LC molecule consists of 30-mer 1, base paired with a complementary 30-mer (1′). Diagnostic restriction sites are represented as follows: E_V, *Eco*RV; R, *Rsa* I; S, *Sma* I; P, *Pvu* II. ψE_I refers to an *Eco*RI-compatible overhang that, upon ligation, does not create an *Eco*RI cleavage site (15). (*c*) Outline of the construction of $J_{ex}(1+3)$. As indicated in *a*, the starting junction consists of 30-mers 1 and 3 and 26-mers 2 and 4. Details of the construction are given in the text. Note: we have found the *Eco*RI–*Hin*dIII fragment (15) to be 159 bp upon resequencing; the *Eco*RI–*Hae* III extension is, therefore, 106 bp.

Construction of the J_{ex} and the LC Molecule. Methods used for the construction and purification of the two-arm J_{ex} were as described (15), with minor modifications (Fig. 1*c*). In the current study, a total of eight oligomers (four 30-mers, and four 26-mer analogues lacking the 5′-AATT sequence) were synthesized for the set of six, two-arm J_{ex}. By annealing appropriate combinations of two 30-mers and two 26-mers, junctions containing two blunt ends and two 5′ overhangs were formed. This modification prevents interjunction interactions between nonextended arms during the birefringence experiments. After ligation of a 159-bp *Eco*RI–*Hin*dIII fragment (15, 24) (at 5–10 molar excess) to the two phosphorylated 5′-AATT junction arms, the extended arms were trimmed back with restriction endonuclease *Hae* III (a single *Hae* III site exists within the 159-bp fragment), leaving 106-bp extensions on two arms of the original junction (Fig. 1*c*). The effective length of the J_{ex} is, therefore, 242 bp. The extended junctions are designated $J_{ex}(i+j)$, where i and j indicate the extended arms according to the numbering scheme depicted in Fig. 1. The secondary structures of the J_{ex} were verified by restriction enzyme digestion, as described (15).

Electric Birefringence Measurements. Birefringence decay (TEB) measurements were performed on a dual-beam birefringence instrument designed by P.J.H.; the components and optical configuration have been described in detail elsewhere (23). The pulse width was set at 2.5 μsec, with a repetition frequency of 0.07 Hz. The cell temperature was maintained at 4.0 ± 0.1°C. The temperature rise during a series of pulses was always ≤0.1°C. Samples were prepared for TEB measurements by resuspending ethanol precipitates of the J_{ex} and LC fragment in the desired buffer, followed by passage of the DNA solution over Sephadex G-25 columns that had been preequilibrated in the same buffer. Final buffer compositions were checked by monitoring the impedance of the birefringence cell. Decay curves were obtained by averaging the results of 8–32 individual measurements, using a Tektronix 7603/7D20 averaging/digitizing oscilloscope. Data were transferred from the Tektronix digitizer through an IBM PC/AT microcomputer to a VAXstation II GPX, where analyses of the full decay curves were carried out using the program CONTIN (25).

Generation of *R*–Θ Plots. Computed ratios, R, of birefringence decay times were determined as a function of the interarm (included) angle, Θ, and persistence length, P, using a modified version of the equilibrium ensemble approach of Hagerman and Zimm (26). The modifications are as follows: (*i*) for each chain, the contour of the helix axis (including both extended and short arms of the junction) was generated using a model in which roll, tilt, and twist were specified for each base pair; (*ii*) ensembles of 1000 chains were used for averaging; (*iii*) for ensembles generated in which individual chains were self-avoiding, chains were rejected from the ensemble if any overlaps were experienced between beads separated by two or more intervening beads. All hydrodynamic computations were carried out on a VAXstation II GPX, using program DIFFROT.

RESULTS

Gel Electrophoretic Behavior of the Two-Arm J_{ex} Under the Conditions Used for TEB Measurements. It has been demonstrated (15) that qualitative information about the structure of the DNA four-way junction can be gleaned from the relative electrophoretic mobilities of the junction, modified by the addition of a 106-bp reporter fragment to two of the four junction arms in all six pairwise combinations. That analysis was carried out at room temperature in E buffer (40 mM Tris acetate/20 mM sodium acetate/1 mM Na_2EDTA, pH 7.9), with and without the addition of 5 mM magnesium acetate. To determine whether the geometry of the junction, as reflected in its electrophoretic behavior, was significantly altered in the low-salt buffer used for the current TEB measurements, we examined the electrophoretic mobilities of the J_{ex} in 10 mM Tris·HCl, pH 8.0/1 mM $MgCl_2$ at 4°C (the conditions used for the current TEB experiments; see Fig. 4). The gel results (Fig. 2) are essentially identical to those obtained in E buffer with 5 mM magnesium acetate (15).

The elongated junctions have also been subjected to electrophoresis in 10 mM Tris·HCl (pH 8.0) with no added magnesium (4°C; data not shown), yielding relative mobilities that are essentially equivalent to those obtained (15) in the absence of magnesium. However, all of the bands are more diffuse and display greater electrophoretic retardation (relative to a *Hae* III digest of pBR322) than do their counterparts in the presence of magnesium. The origin of this general retardation effect is not known but may be a result of increased flexibility at the junction core in the absence of magnesium. The LC molecule has the same electrophoretic

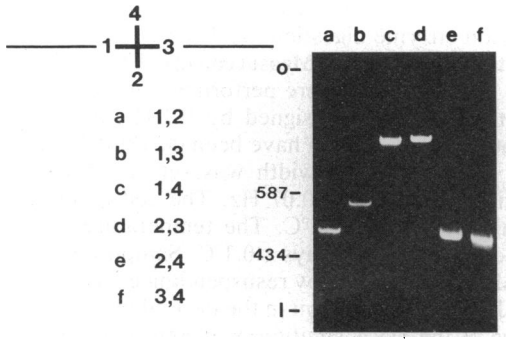

FIG. 2. Polyacrylamide gel electrophoresis of DNA four-way junctions with pairwise combinations of elongated junction arms. Electrophoresis was carried out under buffer conditions identical to those used for the TEB measurements. The key to the left of the gel specifies the pairs of arms that are elongated in each lane of the gel. The numbering convention refers to that of Fig. 1 and ref. 15. Gel markers are as follows: o, origin; I, position of the 242-bp LC; 434 and 587, size markers (bp). Gels contained 6% polyacrylamide [acrylamide/*N,N'*-methylenebisacrylamide, 37:1 (wt/vol)]. The running buffer contained 10 mM Tris·HCl (pH 8.0) and 1 mM $MgCl_2$. The gels were electrophoresed at 4°C and were stained with ethidium bromide prior to visualization on a UV transilluminator.

mobility with respect to the *Hae* III digest of pBR322 under all of the aforementioned conditions.

The Relationship Between Junction Interarm Angle and Birefringence Decay Time. A series of hydrodynamic computations have been performed to determine the relative birefringence decay times, as a function of the interarm (included) angle, of the two-arm J_{ex}. Both computational and experimental results are expressed as the ratio, R, of the junction and LC decay times, τ. In particular, $R(\Theta) = \tau(\Theta)/\tau(180°)$, and $R_{ij} = \tau_{ij}/\tau_{LC}$, where $\tau(\Theta)$ is the computed decay time for a junction having an included angle, Θ; τ_{ij} is the experimental (terminal) decay time of $J_{ex}(i+j)$, and τ_{LC} is the terminal decay time of the LC fragment. The results of the hydrodynamic computations are displayed in Fig. 3, where $R(\Theta)$ is plotted as a function of Θ for several values of the persistence length, P. As expected, the dependence of R on Θ is weakest for included angles greater than 150° or less than 60°. It is also interesting to note that the resultant value for Θ_{ij}, determined from a given experimental value for R_{ij}, is rather insensitive to P for included angles >60°. For example, at 60°, an error in P of ±10% would result in an approximately equivalent error in Θ (±10%). However, for Θ = 90°, the same error in P would result in an error in Θ of <5%. The approach to the determination of all six included interarm angles, therefore, consists of (*i*) experimental determination of all six R_{ij} values from the birefringence decay times, τ_{ij}, of the six two-arm J_{ex} and the LC fragment; (*ii*) determination of P for the LC fragment; and (*iii*) use of the R–Θ plots (Fig. 3) to obtain the six interarm angles.

Determination of the Angles Between Junction Arms in Free Solution. Representative TEB decay curves for J_{ex} in the presence of magnesium (as $MgCl_2$) are displayed in Fig. 4. The terminal decay times, τ_{ij}, for each of the six J_{ex} and the LC fragment, along with the corresponding angles, Θ_{ij}, enclosed by each pair of J_{ex} arms, are listed in Table 1. It is apparent that $J_{ex}(1+4)$ and $J_{ex}(2+3)$ enclose the most acute angles, with $J_{ex}(1+3)$, $J_{ex}(1+2)$, $J_{ex}(2+4)$, and $J_{ex}(3+4)$ enclosing the largest angles (nearest colinearity). The previous conclusion (15), namely, that the oligonucleotide strands comprising the junction are structurally nonequivalent, therefore, is still valid for the junction in free solution. It should be noted (Fig. 4 *Inset*) that the terminal decay times are not influenced by the strength of the previously applied field; consequently, the birefringence decay measurements

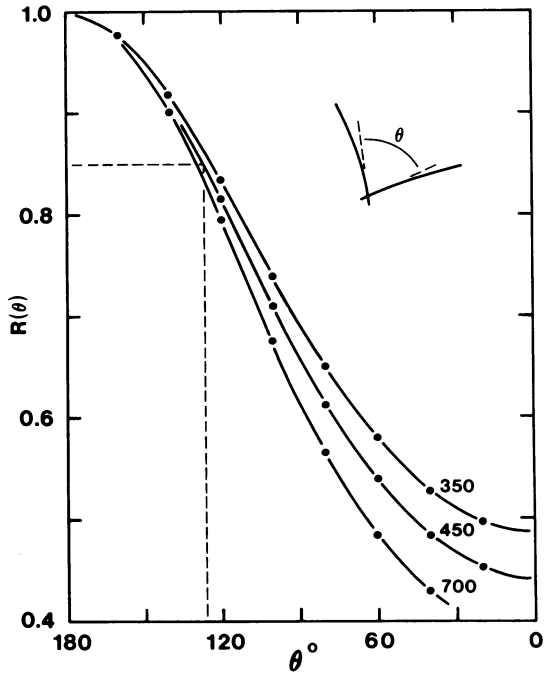

FIG. 3. Dependence of the computed birefringence decay times for J_{ex} on the included angle, Θ, between extended arms. The decay times are normalized to $\tau(\Theta = 180°) = 1.0$ to yield R–Θ plots. R–Θ plots are displayed for three values of the persistence length, $P(A)$, of the control fragment, as indicated in the figure. For the current computations, the interarm angle is located between the central two base-pairs; the short arms are approximated by two beads (15.9 Å per bead) per short arm, and the entire long axis by 26 beads. Three features of the computational model should be noted: (*i*) the contribution of the short arms to τ for Θ = 180° results in an increase in $\tau(180°)$ over τ_{LC} of only 1.3% for P = 500 Å; (*ii*) an uncertainty in the dimension of the junction core as large as ±2 bp would result in an error in $\tau(180°)$ of only 0.5%; and (*iii*) although the displayed curves have not been corrected for chain self-avoidance, the problem of self-avoidance only becomes significant for included angles <60° [for the middle curve, the error in $R(\Theta)$ due to neglect of self-avoidance is 1.0% for Θ = 60°, 6% for Θ = 30°, and 16% for Θ = 0°]. Such errors are well within the limits of experimental uncertainty.

can be related directly to the structures of these molecules in solution.

The Geometry of the Four-Way Junction Shifts upon Removal of Magnesium. The interarm angles were also determined for the junction in the absence of added magnesium; the results of those measurements are presented in Table 2. $J_{ex}(1+4)$ and $J_{ex}(2+3)$ continue to enclose the most acute angles; however, both of these angles are considerably less acute than in the presence of magnesium. Moreover, omission of magnesium appears to decrease the magnitude of the angles enclosed by $J_{ex}(1+2)$, $J_{ex}(1+3)$, $J_{ex}(2+4)$, and $J_{ex}(3+4)$. The arms of the junction thus appear to approach a more uniformly spread arrangement, perhaps reflecting increased flexibility of the junction core in the absence of magnesium (to be distinguished from flexibility in the junction arms themselves, which is reduced). The gel pattern observed by Duckett *et al.* (27) in the absence of magnesium, which would indicate a planar–tetragonal geometry for the junction, is inconsistent with both our gel and solution results. The gel results of those authors may have reflected partial dissociation of their complexes (no stability measurements were reported).

The Relationship Between Electrophoretic Mobility and Interarm Angle Is Not Strictly Monotonic. In Fig. 5, the interarm angles, Θ_{ij}, are plotted as a function of the relative electrophoretic mobilities, R_μ [= μ_{ij}/μ_{LC}], both in the

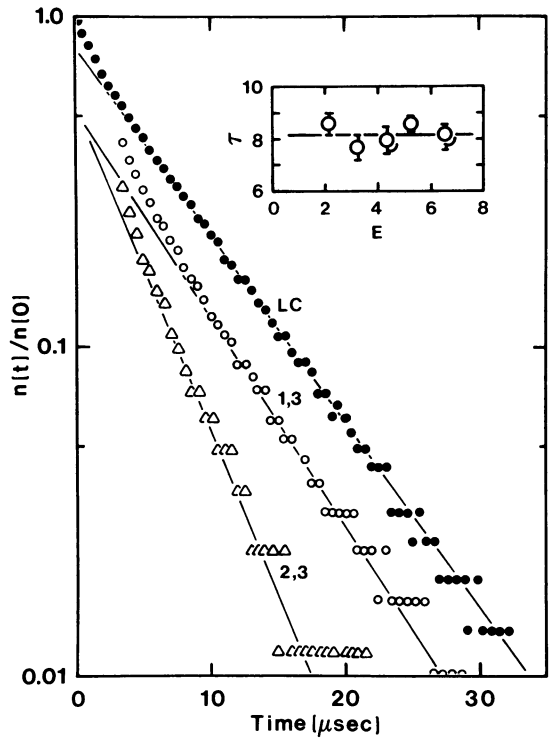

FIG. 4. Birefringence decay of two J_{ex} in $MgCl_2$-containing buffer. Representative semilogarithmic plots of the decay of birefringence $[n(t)/n(0)]$ are given for LC (●), $J_{ex}(1+3)$ (○), and $J_{ex}(2+3)$ (△). Sample solutions contained DNA (90–140 μg/ml), 10 mM Tris·HCl, and 1 mM $MgCl_2$ (pH 8.0). Zero time on the abscissa represents a constant delay of 2.5 μsec after removal of the field. Such a delay permits higher precision of data collection for the terminal portion of the decay curves. (*Inset*) Terminal birefringence decay times, τ(μsec), for $J_{ex}(3+4)$, plotted as a function of the field strength of the orienting pulse. The sample solutions contained DNA (90 μg/ml), and 10 mM Tris·HCl (pH 8.0). The error bars represent ±1 SD in τ_{34}, as determined by the program CONTIN.

presence and absence of added magnesium. Three features of this plot are noteworthy: (*i*) whereas the mobilities of $J_{ex}(1+2)$, $J_{ex}(2+4)$, and $J_{ex}(3+4)$ are approximately twice as large as those of $J_{ex}(1+4)$ and $J_{ex}(2+3)$, both in the presence and absence of magnesium, the range of angles is dramatically reduced in the absence of magnesium; (*ii*) the apparent angles for $J_{ex}(1+3)$ are nearly identical (±Mg), although the corresponding mobilities are distinctly different; and (*iii*) although the relative mobilities of $J_{ex}(1+4)$ are similar (±Mg), the apparent angles differ by ≈2-fold. Thus, relative gel mobilities do not provide an unambiguous measure of relative angles.

Table 1. Rotational decay times and included angles for the J_{ex} in the presence of 1 mM magnesium

Species	τ_{ij}*	R_{ij}†	Θ_{ij}‡
LC	4.55 ± 0.04	1.00	
$J_{ex}(1+2)$	4.43 ± 0.13	0.97	158°
$J_{ex}(1+3)$	4.17 ± 0.17	0.92	140°
$J_{ex}(1+4)$	1.95 ± 0.08	0.43	<50°
$J_{ex}(2+3)$	2.58 ± <0.01	0.57	58°
$J_{ex}(2+4)$	4.63 ± 0.19	1.02	180°
$J_{ex}(3+4)$	4.48 ± 0.13	0.98	161°

*Terminal (longest) decay times (μsec) from CONTIN. All measurements were performed at 4°C; the resulting decay times were corrected to 20°C using the following conversion: $\tau_{20,w} = (\eta_{20,w}/\eta_T) \times [T(K)/293] \times \tau(\text{observed})$. τ_{LC} corresponds to $P = 350$ Å, determined from the current computational model and from the expressions of Hagerman and Zimm (26). This value is somewhat lower than the value of 436 Å (1 mM $MgCl_2$), determined by DNA cyclization (W. H. Taylor and P.J.H., unpublished paper) for a series of molecules (337–350 bp) containing two copies of the 106-bp sequence. The origin of the difference is not completely understood but would have a relatively minor effect on the derived Θ_{ij} values.

†$R_{ij} = \tau_{ij}(\text{mean})/\tau_{LC}(\text{mean})$.

‡Θ_{ij} = angle included between the two elongated junction arms *i* and *j*. Error limits (from τ_{ij} measurements) are displayed in Fig. 5.

Table 2. Rotational decay times and included angles for J_{ex} in the absence of magnesium

Species	τ_{ij}*	R_{ij}	Θ_{ij}†
LC	5.42 ± 0.29	1.00	
$J_{ex}(1+2)$	4.63 ± 0.28	0.85	127°
$J_{ex}(1+3)$	4.81 ± 0.34	0.89	135°
$J_{ex}(1+4)$	4.52 ± 0.47	0.83	123°
$J_{ex}(2+3)$	4.10 ± 0.29	0.76	110°
$J_{ex}(2+4)$	4.96 ± 0.30	0.92	142°
$J_{ex}(3+4)$	4.85 ± 0.39	0.89	135°

*Corrected, as described in the legend to Table 1.

†The included angles were determined using a value for $P = 460$ Å, derived from τ_{LC} as described in the legend to Table 1. Error limits are displayed in Fig. 5.

DISCUSSION

The Structure of the DNA Four-Way Junction in Solution. Sigal and Alberts (3) proposed a model for the structure of the Holliday junction in which pairs of junction arms are coaxially stacked across the junction core. Although certain features of their model may not be entirely relevant to immobile branched structures (15), other aspects of their model may be applicable to the present case. In particular, the close agreement between τ_{LC} and τ_{ij} (for *ij* = 12, 24, and 34) suggests that, in the presence of magnesium, the corresponding junction arms are nearly colinear, increasing the likelihood of stacking interactions across the core. However, in contrast to the Sigal and Alberts model (3), in which the strands comprising the junction are readily interchangable, the current observation argues against appreciable concentrations of distinct structural isomers (28–30) in which alter-

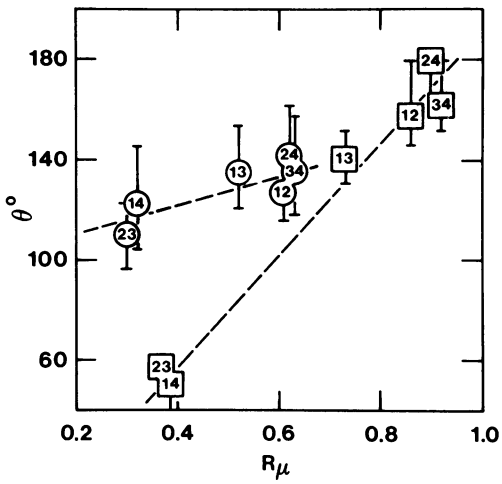

FIG. 5. Plot of the relationship between the relative electrophoretic mobilities, R_μ (= μ_{ij}/μ_{LC}), and the interarm angles, Θ_{ij}, for the six, two-arm J_{ex}, where μ_{ij} is the electrophoretic mobility of $J_{ex}(i+j)$ and μ_{LC} is the corresponding mobility of the LC molecule. Gel conditions are as described in the legend to Fig. 2, except for exclusion of $MgCl_2$ in some experiments. □ , + 1 mM $MgCl_2$; ○, − $MgCl_2$. The numbers enclosed in the symbols represent the positions of the extended arms. The error bars represent the uncertainty in Θ corresponding to ±1 SD in τ_{ij}.

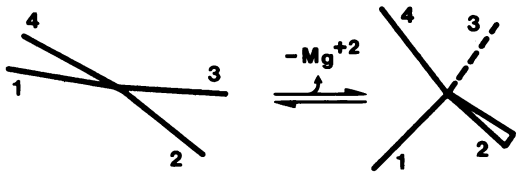

FIG. 6. Schematic representation of the geometries of the four-way junction in the presence and absence of magnesium. The +Mg form of the junction probably has an out-of-plane component.

nate angles are acute, and also rules out a point of significantly increased flexibility at the junction core.

The data presented in Table 1 suggest that the junction may possess an out-of-plane component, as through a partial turn about the bisector of arms 2 and 3 (Fig. 6). Moreover, the inequality, $\Theta_{13} < \Theta_{24}$, suggests an intrinsic asymmetry of the junction. This latter observation further implies that junction geometry is a complex function of sequence. The sequence-dependent nature of junction structure has been verified in several laboratories. Chen *et al.* (29) showed that two junctions, differing only in the base sequence immediately flanking the branch point, manifest opposite hydroxyl radical protection patterns in the vicinity of the junction core. Both the gel electrophoretic experiments of Duckett *et al.* (27) and those performed in our laboratory (unpublished data) demonstrate that changing the base pairs adjacent to the branch point results in changes in the relative gel mobilities of two-arm J_{ex}. If branched intermediates in genetic recombination are cleaved in a biased fashion with respect to the bridging (crossover) strands (27, 29), the geometry of the branched intermediate, itself dictated by junction sequence, may play a major role in determining the outcome of recombinational events.

Interpretation of the Gel Electrophoretic Behavior of Branched DNA Structures. As demonstrated in Fig. 5, a strict monotonic relationship between gel mobility and degree of bending cannot be assumed, and the possibility of some differential deformation of the junction by the gel cannot be ruled out. This point is particularly important for the interpretation of small differences in gel mobility. For example, the conclusion of Duckett *et al.* (27) that junctions are symmetric, coaxially stacked structures was based on fairly small differences in the relative gel mobilities among six pairwise combinations of J_{ex} arms, and on the presumption that equivalent gel mobilities imply equal angles; our results demonstrate that this presumption is not correct. Moreover, those authors assumed, in the absence of any independent evidence, that their fastest-migrating species represented structures having colinear extended arms. This last assumption is unfounded for three reasons: (*i*) all of their J_{ex} are electrophoretically abnormal, (*ii*) the extended arms of their junctions were only 3.3 times longer than the short arms, and (*iii*) since their junction is not directly related to the Seeman and Kallenbach core (13), the conclusions derived from the current study are not directly applicable to their observations. The need for a method to quantify the angles between junction arms in free solution is thus further underscored.

CONCLUSIONS

We have demonstrated that a synthetic DNA four-way junction has a sequence-dependent geometry in free solution, in which pairs of arms are arranged in nearly colinear domains. Determination of the actual angles between junction arms has revealed that the relationship between gel retardation and degree of bending depends on the counterion type. This observation has broad significance inasmuch as similar effects may be occurring in gel systems used to investigate either sequence-dependent or protein-induced curvature of DNA.

The current (TEB) approach should be directly applicable to the study of a wide variety of tertiary structures in RNA as well as DNA. The method provides long-range structural information of a type not readily accessible to x-ray crystallographic or nuclear magnetic resonance methods.

We thank Drs. N. R. Kallenbach and N. C. Seeman for useful discussions concerning this work, Dr. S. Provencher for providing CONTIN, Dr. S. Allison for helpful discussions concerning the use of CONTIN, and V. A. Ramadevi for help with the angle computations and curve-fitting. This study was supported by Grant GM35305 from the National Institutes of Health.

1. Holliday, R. (1964) *Genet. Res.* **5**, 282–304.
2. Broker, T. R. & Lehman, I. R. (1971) *J. Mol. Biol.* **60**, 131–149.
3. Sigal, N. & Alberts, B. (1972) *J. Mol. Biol.* **71**, 789–793.
4. Meselson, M. S. & Radding, C. M. (1975) *Proc. Natl. Acad. Sci. USA* **72**, 358–361.
5. Mizuuchi, K., Kemper, B., Hays, J. & Weisberg, R. A. (1982) *Cell* **29**, 357–365.
6. Lilley, D. M. J. & Kemper, B. (1984) *Cell* **36**, 413–422.
7. deMassy, B., Studier, F. W., Dorgai, L., Appelbaum, E. & Weisberg, R. A. (1984) *Cold Spring Harbor Symp. Quant. Biol.* **49**, 715–726.
8. West, S. C. & Korner, A. (1985) *Proc. Natl. Acad. Sci. USA* **82**, 6445–6449.
9. Symington, L. S. & Kolodner, R. (1985) *Proc. Natl. Acad. Sci. USA* **82**, 7247–7251.
10. Dickie, P., McFadden, G. & Morgan, A. R. (1987) *J. Biol. Chem.* **262**, 14826–14836.
11. Parsons, C. A. & West, S. C. (1988) *Cell* **52**, 621–629.
12. Seeman, N. C. (1982) *J. Theor. Biol.* **99**, 237–247.
13. Seeman, N. C. & Kallenbach, N. R. (1983) *Biophys. J.* **44**, 201–209.
14. Kallenbach, N. R., Ma, R.-I. & Seeman, N. C. (1983) *Nature (London)* **305**, 829–831.
15. Cooper, J. P. & Hagerman, P. J. (1987) *J. Mol. Biol.* **198**, 711–719.
16. Wemmer, D. E., Wand, A. J., Seeman, N. C. & Kallenbach, N. R. (1985) *Biochemistry* **24**, 5745–5749.
17. Wu, H.-M. & Crothers, D. M. (1984) *Nature (London)* **308**, 509–513.
18. Hagerman, P. J. (1984) *Proc. Natl. Acad. Sci. USA* **81**, 4632–4636.
19. Diekmann, S. & Wang, J. C. (1985) *J. Mol. Biol.* **186**, 1–11.
20. Fredericq, E. & Houssier, C. (1973) *Electric Dichroism and Electric Birefringence* (Clarendon, Oxford, U.K.).
21. Hagerman, P. J. (1981) *Biopolymers* **20**, 1503–1535.
22. Elias, J. G. & Eden, D. (1981) *Macromolecules* **14**, 410–419.
23. Hagerman, P. J. (1985) *Methods Enzymol.* **117**, 198–219.
24. Taylor, W. H. & Hagerman, P. J. (1987) *Gene* **53**, 139–144.
25. Provencher, S. W. (1982) *Comput. Phys. Commun.* **27**, 229–242.
26. Hagerman, P. J. & Zimm, B. H. (1981) *Biopolymers* **20**, 1481–1502.
27. Duckett, D. R., Murchie, A. I. H., Diekmann, S., von Kitzing, E., Kemper, B., & Lilley, D. M. J. (1988) *Cell* **5**, 79–89.
28. Mueller, J. E., Kemper, B., Cunningham, R. P., Kallenbach, N. R. & Seeman, N. C. (1988) *Proc. Natl. Acad. Sci. USA* **85**, 9441–9445.
29. Chen, J.-H., Churchill, M. E. A., Tullius, T. D., Kallenbach, N. R. & Seeman, N. C. (1988) *Biochemistry* **27**, 6032–6038.
30. Churchill, M. E. A., Tullius, T. D., Kallenbach, N. R. & Seeman, N. C. (1988) *Proc. Natl. Acad. Sci. USA* **85**, 4653–4656.